Pak. j. sci. ind. res. Ser. A: phys. sci. 2013 **56** (2) 59-69

Cyclic Voltammetric Studies of Thymoquinone with Iron (III)

Farah Kishwar* and Qamar-ul-Haq
Department of Chemistry, Federal Urdu University of Arts, Science and Technology,
Gulshan-e-Iqbal Campus, Karachi-75300, Pakistan

(received November 28, 2012; revised February 11, 2013; accepted March 6, 2013)

Abstract. Complexation of thymoquinone an active ingredient of *Nigella sativa*, with Fe(III) has been analyzed using cyclic voltammetry. This electrochemical study was performed at glassy carbon as working electrode, platinum as auxiliary and saturated calomel as reference electrode. Whole work was performed at 25±1 °C in aqueous medium using NaCl as supporting electrolyte. Present study reflects effects of scan rates, concentrations, ratios and successive cyclic scans on Fe(III)-thymoquinone complex. Results revealed that the complex shows quasi-reversible electron transfer process. E° of complex was found to be 0.271± 0.030 V whereas diffusion coefficient was 9.178×10^{-5} cm^2s^{-1}. The values of transfer coefficients, α and β were also determined. The value of α was found to be 0.786±0.01-0.923±0.02 whereas value of β was found in the range of 0.813±0.01-1.021±0.01. Calibration curve method with linear regression line confirms that cyclic voltammetry can be used for quantification of Fe(III)-thymoquinone complex for pharmaceutical assay.

Keywords: thymoquinone, iron (III), cyclic voltammetry, Quasi-reversible behaviour, Randles-Sevick equation

Introduction

Thymoquinone (2-methyl-5-isopropyl-1,4-benzoquinone) (TQ) is the major component of the essential oil of *Nigella sativa*, but it is also present in the fixed oil of the seed (Ali and Blunden, 2003) and it is an active principle responsible for many of the seed's beneficial effects (Mehta *et al*., 2009; Xin *et al*., 2008). Among various bioactivities, examined for TQ, one of the most important is its antioxidant activity (Badary *et al*., 2003; Mansour *et al*., 2002). The compound has been observed to decrease cellular oxidative stress (Mohamed *et al*., 2003) and has a potent chemo-preventive potential of inhibiting the process of carcinogenesis (Badary *et al*., 2007; Badary *et al*., 1999). In addition, several research studies have shown its other pharmacological activities such as anti-inflammatory (Syed, 2008; Gazzar *et al*., 2007), anti-tumor (Gali-Muhtasib *et al*., 2008; Shoieb *et al*., 2003), antidiabatic (Abdelmeguid *et al*., 2010; Fararh *et al*., 2005), antitussive (Hosseinzadeh *et al*., 2008), antimicrobial (Mouhajir *et al*., 1999), apoptosis induction (El-Mahdy *et al*., 2005) and neuro-protective (Al-Shabanah *et al*., 1998) activities.

Structurally, TQ (Fig. 1) belongs to 2,5-di-substituted benzoquinone class of compounds having methyl and isopropyl groups at carbon-2 and carbon-5, respectively (Padhye *et al*., 2008). TQ can be prepared by oxidation of thymol (Dockal *et al*., 1955). The crystal structure of TQ has been determined using high-resolution X-ray powder diffraction, which showed that TQ belongs to the triclinic system. Weak Vander Walls forces have been found in the molecules by thermal analysis (Pagola *et al*., 2004).

Iron is the second most abundant metal after aluminium and the fourth most abundant element in the earth's crust. The earth's core is believed to consist mainly of iron and nickel (Cotton and Wilkinson, 1988). Iron has a key role in our life also, as it is an essential component of several proteins and enzymes. Iron can serve different functions because of the fact that it can exist in two different ionic states, ferrous and ferric iron, e.g., it can

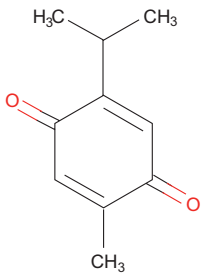

Fig. 1. Structure of thymoquinone.

*Author for correspondence; E-mail: farahkishwar@yahoo.com

serve as a cofactor to enzymes involved in oxidation-reduction reactions. Iron forms a part of the electron carriers that participate in the electron transport chain. In the final step, these carrier transport hydrogen and electrons form energy-yielding nutrients to oxygen, forming water, and in the process make ATP. Most of the body's iron is found in two proteins: hemoglobin in the red blood cells and myoglobin in the muscle cells. In both iron helps to accept, carry and then release oxygen. Iron is also required by enzymes, which are involved in the making of amino acids, collagen, hormones and neurotransmitters (Eleanor and Sharon, 2002).

Iron (III) forms complexes with a number of ligands such as; chloride, fluoride, cyanide, amines etc., but oxygen containing ligands have high affinity for it. Iron (III) also forms complexes with oxalate and phosphate ion, glycerol and sugars etc. Formation of oxo and/or hydroxo bridges is one of its characteristic features (House croft and Sharpe, 2005). Iron (III) in aqueous solution has tendency to hydrolyze and form complexes such as $[Fe(H_2O)_6]^{3+}$(Cotton and Wilkinson, 1988). Regarding stability, iron (II) and iron (III) lie much closer together as compared to (II) and (III) oxidation states of other transition elements. This is the reason that ferrous (Fe^{2+}) and ferric (Fe^{3+}) ions are readily inter-convertible by the use of mild oxidizing or reducing agents. The standard electrode potential of Fe^{2+}/Fe^{3+} ($E°=0.77$) shows that iron (III) is a good oxidizing agent (House croft and Sharpe, 2005).

Since most of the biological activities of TQ are due to its antioxidant behaviour, its electrochemical study is very important. Although polarographic behaviour of TQ has been examined (Michelitsch and Rittmannsberger, 2003), which shows a single reversible peak, not much work is done on electrochemical study of complexes of TQ. Keeping this point in view electrochemical study of complex of TQ with iron has been performed.

Materials and Methods

Reagents and glassware. All reagents used were of analytical grade, purchased from Merck, and MP Biochemicals LLC. All glassware used were of standard quality, properly cleaned and rinsed with distilled-deionized water before use. For cyclic voltammetric studies ferric chloride (hexa hydrate), thymoquinone (TQ) and sodium chloride were used.

Instrumentation. ***Cyclic voltammeter.*** CHI-760 D Electrochemical work station, cyclic voltammeter was used for electrochemical studies. The instrument consists of a computer under Windows environment, a potentiostat and a cell assembly. The cell assembly consisted of a cell stand and a cyclic voltammetric (CV) glass cell. There were three electrodes, a glassy carbon electrode as working electrode, a saturated calomel electrode as reference electrode and a platinum wire electrode as an auxiliary or counter electrode. Repolishing and resurfacing of working electrode was done time to time, especially when supporting electrolyte or analyte was changed. Alumina polishing compound was used to polish working electrode. Then the electrode was thoroughly washed with distilled water in order to remove alumina compound from its surface. Finally, nitrogen purging was checked for the system, but its presence or absence was found to produce no change in voltammograms, so all experimental work was performed without nitrogen.

Sample preparation. ***Supporting electrolyte solution.*** In a 500 mL volumetric flask 2.9220 g of NaCl was taken then dissolved in distilled deinoized water to prepare 0.1 M solution of NaCl.

Analyte solutions. 0.005M solution of TQ and equimolar solution of ferric chloride were prepared as analyte by taking sodium chloride (0.1 M) as electrolyte solution.

Cyclic voltammetric studies. Fresh solutions of analyte and supporting electrolyte were prepared every time. The cell assembly was rinsed thrice with the analyte every time and the working electrode was repolished time to time throughout the experiment. First of all, the base-line of the supporting electrolyte was taken and then 15.0 mL of analyte was run to get overlay of NaCl (0.1 M), Fe(III) solution (5×10^{-4} M), TQ (5×10^{-4} M) and Fe(III) – TQ (5×10^{-4} M). The scan rate was 0.1 V and current sensitivity was 1×10^{-4} A/V. The potential range was set from -0.20 V to + 0.80 V and then reversed back to -0.20 V. The complexation of Fe(III) and TQ was studied in the light of effects of several parameters such as, effect of metal ligand ratio, effect of scan rate, effect of concentration and effect of repeated scan.

To check effect of metal-ligand ratio on complexation, complex solutions having metal ligand ratios 1:1 to 1:4 were prepared. To study the effect of concentration, complex solutions having concentrations 0.02×10^{-3}, 0.1×10^{-3}, 0.2×10^{-3}, 0.4×10^{-3}, 0.6×10^{-3}, 0.8×10^{-3}, 1.0×10^{-3} and 1.2×10^{-3} M were prepared. In order to examine effect of scan rate Fe(III)-TQ complex was analyzed at different scan rates ranging 0.05-200 V by keeping all parameters constant. Repeated scan of the complex of Fe(III) and TQ was also recorded up to 14 sweep segments. The metal-ligand ratio of the complex solution for the effect of concentration, scan rate and repeated scan was 1:3.

Results and Discussion

Cyclic voltammetric study of Fe(III)-thymoquinone complex revealed valuable information which is as follows:

Confirmation of complex formation. Complex formation was checked by comparing voltammograms of supporting electrolyte NaCl (0.1M), Fe(III) (5×10^{-4} M), thymoquinone (5×10^{-4} M) and Fe(III)-thymoquinone complex(1:1) (5×10^{-4} M) (Table 1, Fig. 2a-d). Analysis was performed at 0.1 V/sec at current sensitivity 1×10^{-4} A/V. Linearity in baseline confirms absence of impurity and cleanliness of working electrode (Fig. 2a). Fe(III)-thymoquinone complex showed anodic and

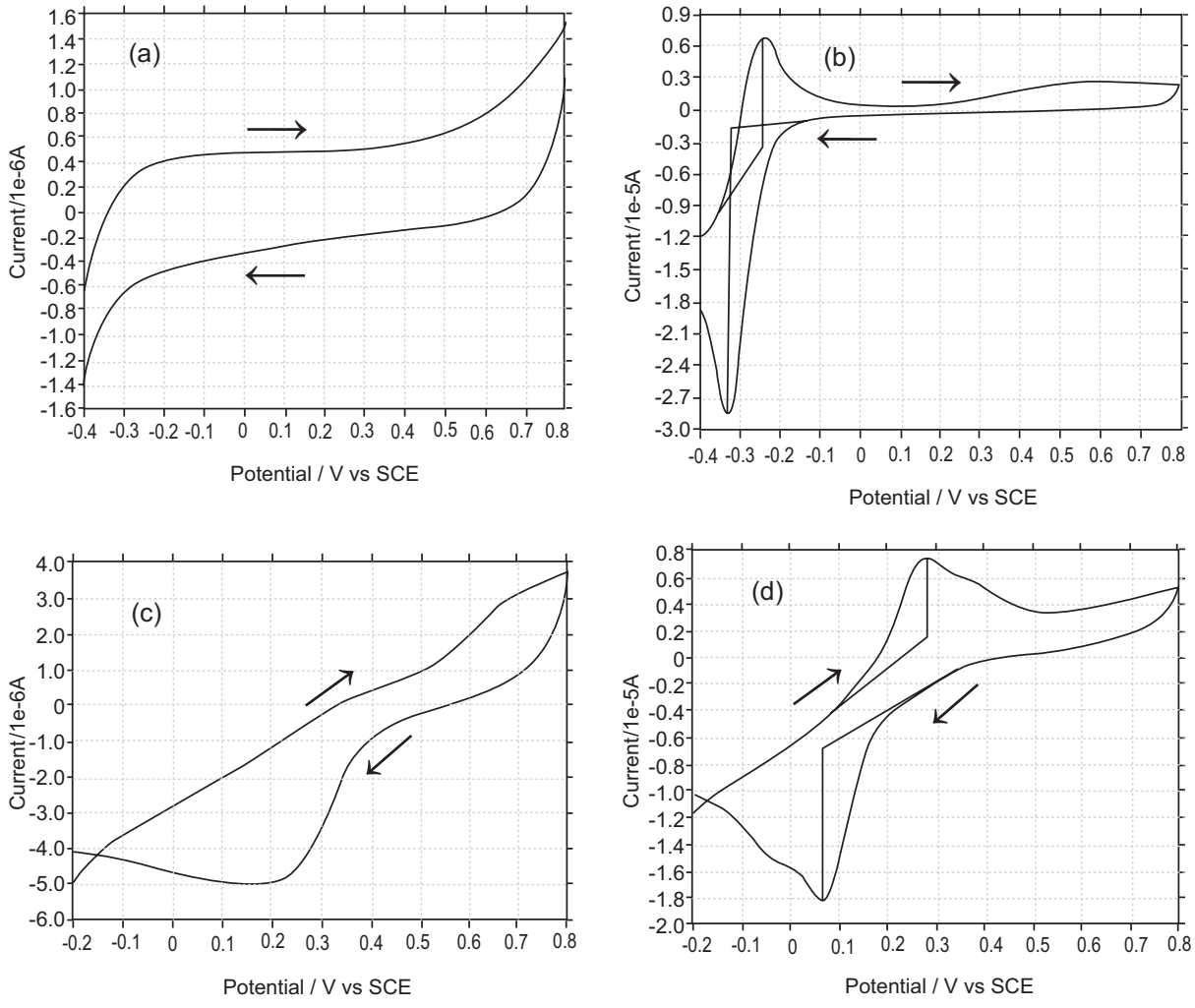

Fig. 2a-d. Cyclic voltammograms of (a) NaCl (0.1 M), (b) thymoquinone (5×10^{-4} M), (c) Fe(III) (5×10^{-4} M) and (d) Fe(III)-thymoquinone complex (5×10^{-4} M) at 0.1 V/s.

cathodic peaks at 0.282 V and 0.066 V, respectively. Neither Fe(III) nor thymoquinone showed peaks within this potential range which clearly indicates that complex formation has occurred in aqueous medium (Table 1, Fig. 2a-d).

Effect of scan rate on voltammograms of Fe(III)-thymoquinone complex. Effect of scan rate from 0.05 V/s to 0.2 V/s was analyzed on Fe(III)-thymoquinone complex (1:3) (5×10^{-4} M) and different electrochemical parameters E_{pa}, E_{pc}, I_{pa}, I_{pc} etc. were determined (Table 2, Fig. 3). Voltammograms fulfill the criteria of quasi-reversible behaviour (Table 3) because by increasing scan rates anodic peak potential shifts from 0.298 V to 0.326 V. Similarly cathodic peak shifted from 0.049 V to 0.018 V. Another quasi-reversible behaviour found was that I_{pa}/I_{pc} was not equal to 1. Furthermore, E_{pa}-E_{pc} was observed greater than 59/n mV and it increased with the increase in ν. I_p was also found to increase with $\nu^{1/2}$ (Fig. 4). Negative shift of E_{pc} with increase of ν further favours the quasi-reversible behaviour (Table 2 and 3). Plot of the peak potential against log of scan rates gave very good R^2 values (Fig.5). The values of α and β were also determined using the relation $0.048/(E_p-E_{p/2})$. Values of α and β at

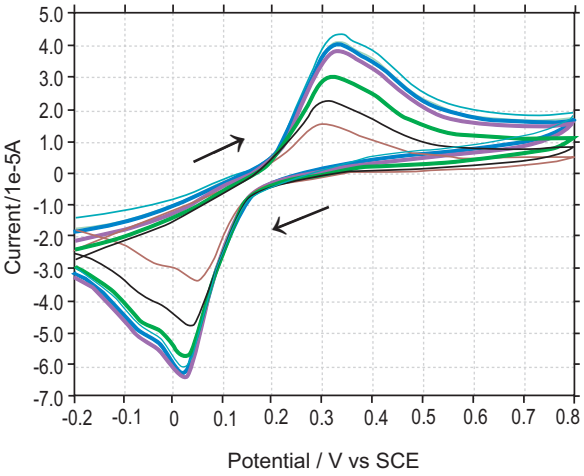

Fig. 3. Cyclic voltammograms of Fe(III)-thymoquinone complex at different scan rates (0.05 V, 0.1 V, 0.15 V, 0.2 V).

Table 1. Electrochemical parameters of cyclic voltammograms of thymoquinone, Fe(III), and Fe(III)-thymoquinone complex

Component/Complex	I_{pa} (A)	I_{pc} (A)	E_{pa} (V)	E_{pc} (V)
Thymoquinone	$1.017\times10^{-5}\pm0.01$	$2.717\times10^{-5}\pm0.01$	-0.242±0.01	-0.326±0.01
Fe(III)	-	-	-	-
Fe(III)-thymoquinone complex	$5.875\times10^{-6}\pm0.01$	$1.149\times10^{-5}\pm0.01$	0.282±0.01	0.066±0.01

Table 2. The values of E_p, $E_{p/2}$, E_p-$E_{p/2}$, E_{pa}-E_{pc} and I_p from cyclic voltammograms of Fe(III)-thymoquinone complex with different scan rates

Scan rate (V/s)	E_{pa} (V)	$E_{pa/2}$ (V)	E_{pa}-$E_{pa/2}$ (V)	I_{pa} $\times10^{-5}$(A)	I_{pa}/I_{pc}	βn_b $=0.048/E_{pa}$-$E_{pa/2}$
0.05	0.298 ± 0.01	0.25 ± 0.01	0.048 ± 0.011	0.798 ± 0.01	0.274 ± 0.01	1.00 ± 0.01
0.10	0.309 ± 0.01	0.26 ± 0.01	0.049 ± 0.011	1.035 ± 0.01	0.253 ± 0.01	1.021 ± 0.01
0.15	0.318 ± 0.01	0.266 ± 0.01	0.052 ± 0.011	1.743 ± 0.01	0.355 ± 0.01	0.923 ± 0.01
0.20	0.326 ± 0.01	0.269 ± 0.01	0.057 ± 0.011	2.541 ± 0.01	0.463 ± 0.01	0.842 ± 0.01

Scan rate (V/s)	E_{pc} (V)	$E_{pc/2}$ (V)	E_{pc}-$E_{pc/2}$ (V)	E_{pa}-E_{pc} (V)	I_{pc} $\times10^{-5}$(A)	αn_a $=0.048/E_{pc}$-$E_{pc/2}$
0.05	0.049 ± 0.01	0.11 ± 0.01	-0.061 ± 0.011	0.249 ± 0.01	2.917 ± 0.01	0.786 ± 0.01
0.10	0.034 ± 0.01	0.09 ± 0.01	-0.056 ± 0.011	0.275 ± 0.01	4.084 ± 0.01	0.857 ± 0.01
0.15	0.024 ± 0.01	0.082 ± 0.01	-0.058 ± 0.011	0.294 ± 0.01	4.912 ± 0.01	0.828 ± 0.01
0.20	0.018 ± 0.01	0.076 ± 0.01	-0.058 ± 0.012	0.308 ± 0.01	5.488 ± 0.01	0.828 ± 0.01

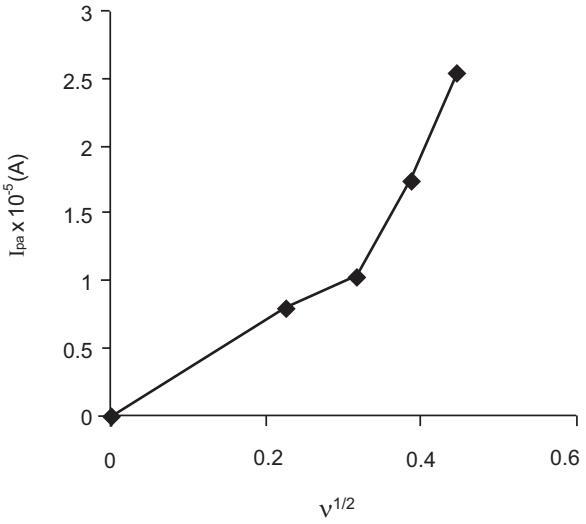

Fig. 4. Variations of anodic and cathodic peak current with square root of sweep rate from the cyclic voltammograms of Fe(III)-thymoquinone complex.

different scan rates were found 0.786 ± 0.01-0.923 ± 0.02 and 0.813 ± 0.01-1.021 ± 0.01, respectively.

Effect of concentration on voltammograms of Fe(III)-thymoquinone complex. Effect of concentration was judged by calibration curve method. To understand the effect of concentration for current study Randles-Sevcik equation is helpful as given below:

$$I_p = 0.4463\ nFACo^*\ (nF\nu D^\circ/RT)^{1/2}$$

Where:

I_p = peak current (A)
ν = scan rate (V/s)
n = Number of electron transfer
F = Faraday's constant
A = Area of electrode (cm^2)
Co* = Concentration of Fe(III)-thymoquinone complex (moles/cm^3)
D^0 = Diffusion coefficient of Fe(III)-thymoquinone complex ($cm^2\ s^{-1}$)
T = 25 ± 2 °C
R = Rate constant

More precisely this equation can be written as follows:

$$I_p = (2.69\times10^5)\ D^{1/2}(n)^{3/2}\ AC\ (\nu)^{1/2}$$

Effect of concentration (0.02×10^{-3} M to 1.2×10^{-3} M) followed Randles-Sevcik equation, because current was directly proportional to concentration (Fig. 6). Calibration curve along with least square fit line showed no major deviation from zero. So no adsorption occurred on electrode surface. These results indicate that calibration curve method can be used for quantification of Fe(III)-thymoquinone complex

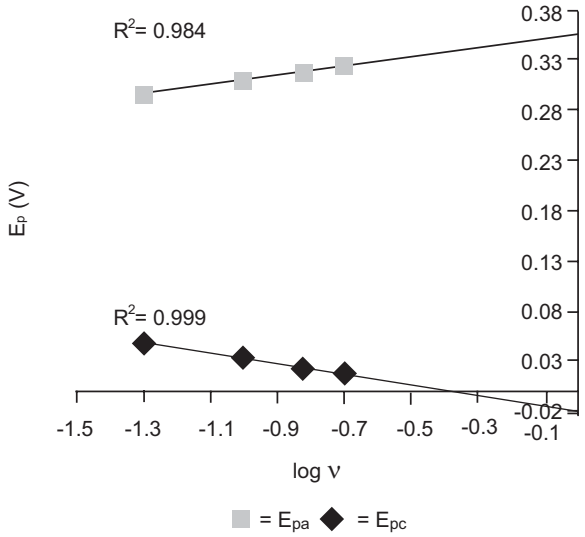

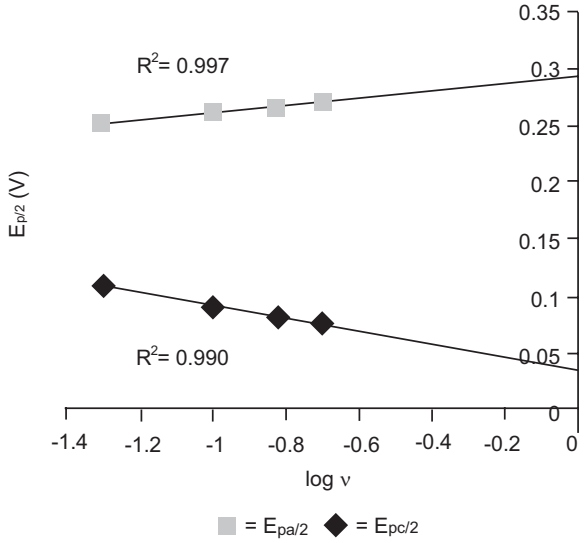

Fig. 5. Variation of anodic and cathodic peak potentials with sweep rate from cyclic voltammograms of Fe(III)-thymoquinone complex.

Table 3. Comparison of diagnostic criteria for reversible, irreversible and quasi-reversible systems at 25±1 °C and results obtained from Fe(III)- thymoquinone complex

S.No.	Comparison of diagnostic criteria	Results obtained from Fe(III)-thymoquinone complex
	Criteria for reversible system*	
1	$\|I_p\| \alpha \nu^{1/2}$	$\|I_p\|$ is not proportional to $\nu^{1/2}$
2	$\|I_{pa} / I_{pc}\| = 1$	$\|I_{pa} / I_{pc}\| \neq 1$
3	$\Delta E_p = E_{pa}-E_{pc} = 59/n$ mV	$\Delta E_p = E_{pa}-E_{pc} > 59/n$ mV and increases as ν increases
4	E_p is independent of ν	E_p is dependent of ν
5	$\|E_p-E_{p/2}\| = 59/n$ mV	$\|E_p-E_{p/2}\| \neq 59/n$ mV
	Criteria for irreversible system*	
1	$\|I_{pc}\| \alpha \nu^{1/2}$	$\|I_{pc}\| \alpha \nu^{1/2}$
2	No reverse peak	Reverse peak is present
3	E_{pc} shifts $-30/\alpha_c n_\alpha$ mV for each decade increase in ν	E_{pc} shift $\neq -30/\alpha_c n_\alpha$ mV for each decade increase in ν
4	$\|E_p-E_{p/2}\| = 48/\alpha_c n_\alpha$ mV	$\|E_p-E_{p/2}\| \neq 48/\alpha_c n_\alpha$ mV
	Criteria for Quasi-reversible system**	
1	$\|I_p\|$ is not proportional to $\nu^{1/2}$, but increases with increase in $\nu^{1/2}$	$\|I_p\|$ increases with increase in $\nu^{1/2}$
2	$\|I_{pa}/I_{pc}\| = 1$, provided $\alpha_c = \alpha_a = 0.5$	$\|I_{pa}/I_{pc}\| \neq 1$
3	$E_{pa}-E_{pc} > 59/n$ mV and increases with increase in ν	$E_{pa}-E_{pc} > 59/n$ mV and increases with increase in ν
4	E_{pc} shifts negatively as ν increases	As ν increases E_{pc} shifts negatively

References* = (Greef *et al*., 1985); References** = (Bard and Faulkner, 2004; Greef *et al*., 1985; Nicholson, 1965).

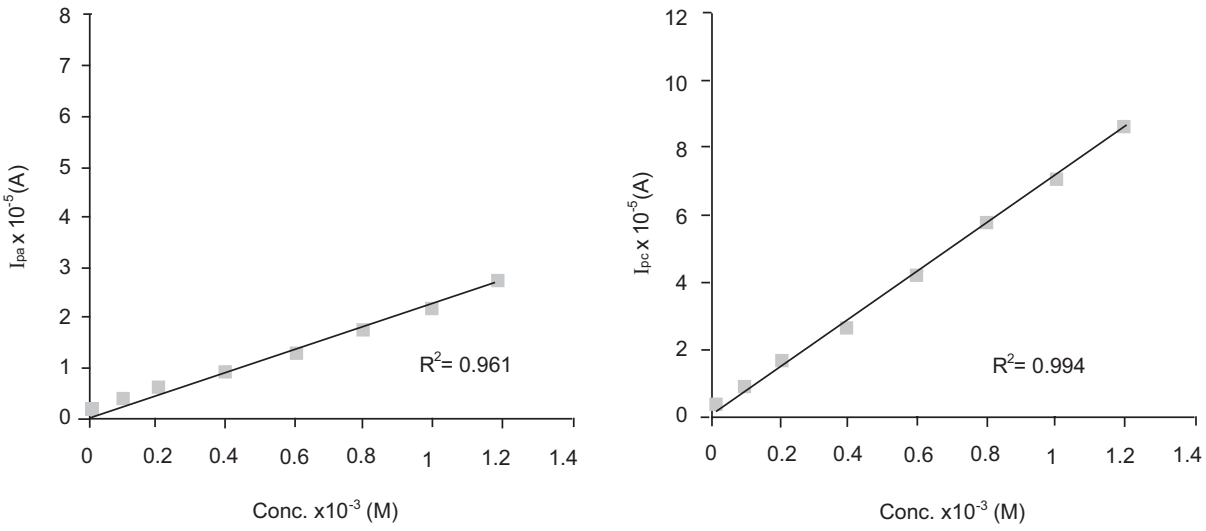

Fig. 6. Plot of anodic and cathodic peak current against concentration of Fe(III)-thymoquinone complex.

within a wide range i.e. (0.02×10^{-3} M to 1.2×10^{-3} M).

Effect of concentration on peak potential (E_{pa}) gives a straight line similarly $E_{pc/2}$ against log of concentration also shows a straight line with good R^2 value (Fig. 7).

Effect of ratio. Here as well, cyclic voltammograms followed the criteria for quasi-reversible reactions because I_{pa}/I_{pc} was not equal to one and $E_{pa}-E_{pc}$ showed values greater than 59/n mV and it increased with the increase in ν. The values of α and β were found in the range of 0.827 ± 0.01 to 0.923 ± 0.02 and 0.842 ±

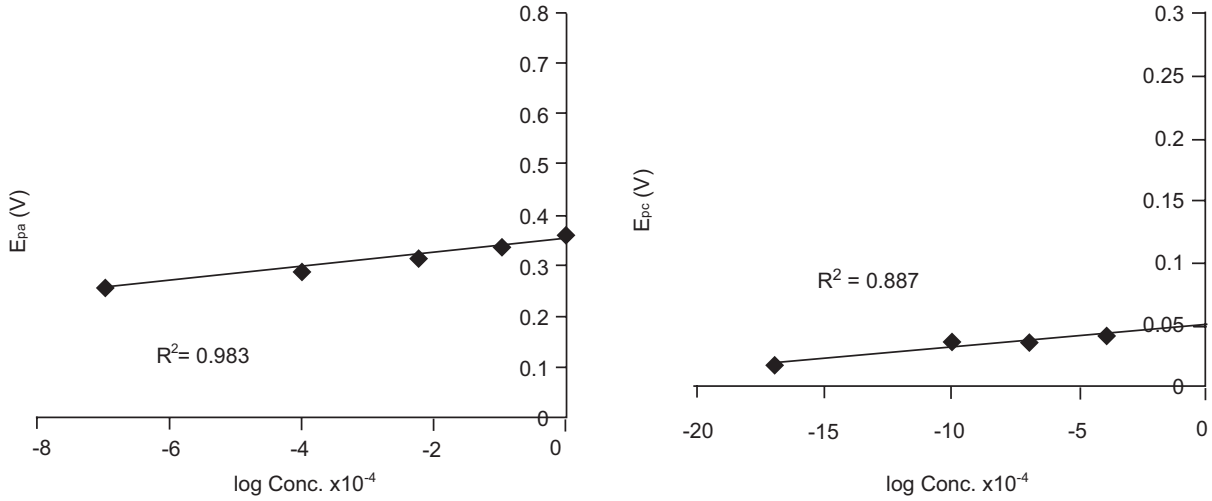

Fig. 7. Variation of anodic and cathodic peak potential with log of concentration on cyclic voltammogram of Fe(III)-thymoquinone complex.

0.01 to 0.979 ± 0.01, respectively (Table 4). Effect of metal ligand ratio on peak potential (E_{pa} and E_{pc}) gave a straight line, similarly the plot of $E_{p/2}$ against M: L ratio also gave a straight line with good R^2 value (Fig. 8).

It was found that by increasing the ratio I_{pa} become approximately constant at 1:3 metal to ligand ratio which may be due to maximum complexation at this ratio (Table 4, Fig. 9).

Effect of repeated scan. Effect of repeated scan on Fe(III)-thymoquinone complex was analyzed up to 14 repeated scans in aqueous medium (NaCl) (Fig. 10). Results revealed that the shape of the cyclic voltammograms of complex remain unchanged in terms of peak potentials (E_{pa} and E_{pc}) but a little bit change in anodic and cathodic peak heights was noticed in these cycles, however, only up to 3rd to 4th cycle limiting values were achieved. The shape of single and multiple scan was similar which confirms neither adsorption nor deposition of complex on electrode surface.

Analysis of diffusion coefficient for Fe(III)-thymoquinone complex. Cyclic voltammetry is a cheap and easy technique for the determination of diffusion coefficient of different complexes and compounds (Anwer, 2006; Ali, 1995). So present study has used cyclic voltammetry for calculation of diffusion coefficient of Fe(III)-thymoquinone complex. For this

Table 4. The values of E_p, $E_{p/2}$, E_{pa}-E_{pc}, I_p and αn_a and βn_b from cyclic voltammograms of Fe(III)-thymoquinone complex with different metal-ligand ratios

Ratio L/M	$E_{pa/2}$ (V)	E_{pa}-$E_{pa/2}$ (V)	I_{pa}/I_{pc}	β_{nb} = 0.048/ E_{pa}-$E_{pa/2}$
1	0.23 ± 0.03	0.052 ± 0.03	0.511	0.923 ± 0.01
2	0.241± 0.01	0.057 ± 0.01	0.343	0.842 ± 0.01
3	0.26 ± 0.01	0.049 ± 0.01	0.253	0.979 ± 0.01
~~4~~	~~0.27 ± 0.02~~	~~0.051 ± 0.02~~	~~0.237~~	~~0.941 ± 0.02~~
Ratio L/M	$E_{pc/2}$ (V)	E_{pc}-$E_{pc/2}$ (V)	E_{pa}-E_{pc} (V)	α_{na} = 0.048/ E_{pa}-$E_{pa/2}$
1	0.12 ± 0.01	-0.054 ± 0.01	0.216 ± 0.01	0.889 ± 0.01
2	0.1 ± 0.01	-0.052 ± 0.02	0.25 ± 0.02	0.923 ± 0.02
3	0.09 ± 0.01	-0.056 ± 0.01	0.275 ± 0.01	0.857 ± 0.01
4	0.08 ± 0.02	-0.058 ± 0.02	0.299 ± 0.02	0.827 ± 0.01

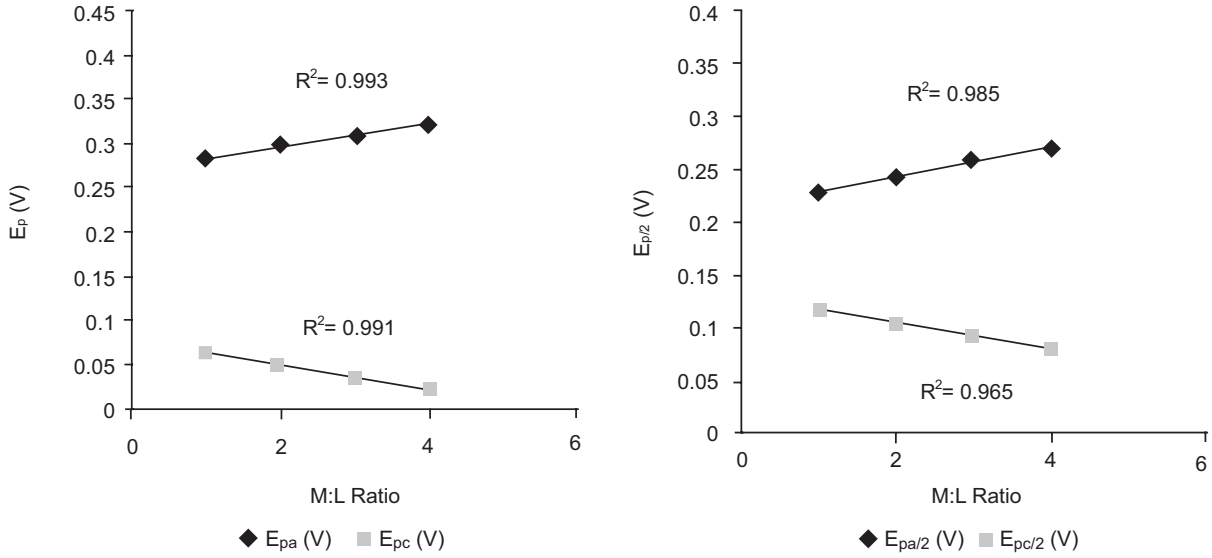

Fig. 8. Variation of anodic and cathodic peak potential with change of metal-ligand ratio in cyclic voltammograms of Fe(III)-thymoquinone complex.

purpose diffusion coefficient of the complex was determined using Randles- Sevcik (Greef *et al*., 1985) equation by varying scan rates, concentrations and metal-ligand ratios (Table 5a-c). Its value was found to be approximately same and no reasonable effect of varying scan rates, concentration or metal-ligand ratio was observed. Area of electrode (A) was 0.0706 cm^2 whereas number of electron transfer (n) was 1.

Analysis of E°, a characteristic property. E° (the potential corresponding to 85% of the peak current) is a characteristic property and is constant for a particular system. Effects of scan rate, concentration and ratio were observed on E° and it was found to be constant at all scan rates, concentration and ratios (Table 6).

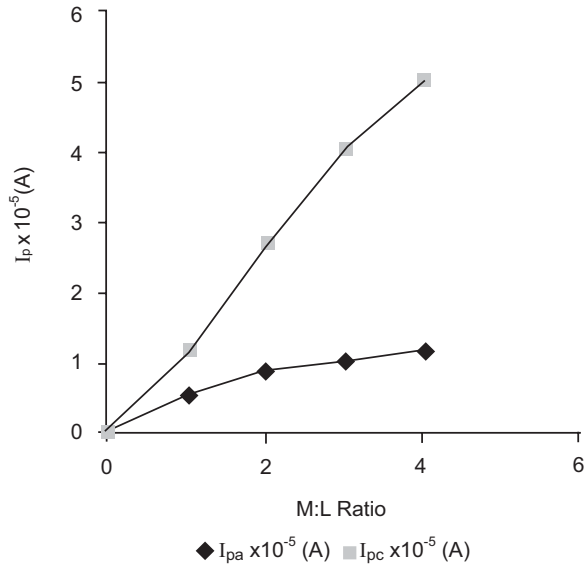

Fig. 9. Variation of anodic and cathodic peak currents with change of metal-ligand ratio in cyclic voltammograms of Fe(III)-thymoquinone complex.

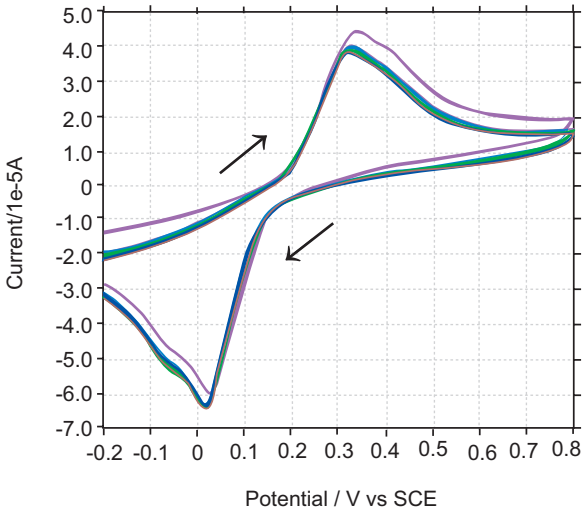

Fig. 10. Repeated scan cyclic voltammograms of Fe(III)-thymoquinone (1:3) complex at 0.1 V.

Table 5a. Diffusion coefficients of the Fe(III)-thymoquinone complex at different scan rates $D^{1/2} = I_p/(2.69\times10^5)(n)^{3/2}\ AC\ (\nu)^{1/2}$

ν (V/s)	$\nu^{1/2}$	I_{pa} $\times10^{-5}$(A)	$D^{1/2}$	D ($cm^2\ s^{-1}$)
0.05	0.224	0.798 ± 0.01	3.572×10^{-3}	1.408×10^{-5}
0.10	0.316	1.035 ± 0.01	3.449×10^{-3}	1.189×10^{-5}
0.15	0.387	1.743 ± 0.01	4.743×10^{-3}	2.25×10^{-5}
0.20	0.447	2.541 ± 0.01	5.986×10^{-3}	3.583×10^{-5}
ν (V/s)	$\nu^{1/2}$	I_{pc} $\times10^{-5}$ (A)	$D^{1/2}$	D ($cm^2\ s^{-1}$)
0.05	0.224	2.917 ± 0.01	1.371×10^{-2}	1.880×10^{-4}
0.10	0.316	4.084 ± 0.01	1.361×10^{-2}	1.852×10^{-4}
0.15	0.387	4.912 ± 0.01	1.34×10^{-2}	1.796×10^{-4}
0.20	0.447	5.488 ± 0.01	1.292×10^{-2}	1.669×10^{-4}

Table 5b. Diffusion coefficients of Fe(III)-thymoquinone complex at different concentrations

Conc. (M)	I_{pa} $\times10^{-5}$ (A)	$D^{1/2}$	D ($cm^2\ s^{-1}$)
0.1×10^{-3}	0.4839 ± 0.01	8.064×10^{-3}	6.503×10^{-5}
0.2×10^{-3}	0.7272 ± 0.01	6.06×10^{-3}	3.672×10^{-5}
0.4×10^{-3}	0.9398 ± 0.01	3.916×10^{-3}	1.533×10^{-5}
0.6×10^{-3}	1.188 ± 0.01	3.299×10^{-3}	1.088×10^{-5}
0.8×10^{-3}	1.735 ± 0.01	3.614×10^{-3}	1.306×10^{-5}
1.0×10^{-3}	2.199 ± 0.01	3.664×10^{-3}	1.342×10^{-5}
1.2×10^{-3}	2.788 ± 0.02	3.871×10^{-3}	1.498×10^{-5}
Conc. (M)	I_{pc} $\times10^{-5}$ (A)	$D^{1/2}$	D ($cm^2\ s^{-1}$)
0.1×10^{-3}	1.007 ± 0.01	1.678×10^{-2}	2.816×10^{-4}
0.2×10^{-3}	1.738 ± 0.01	1.448×10^{-2}	2.097×10^{-4}
0.4×10^{-3}	2.582 ± 0.01	1.076×10^{-2}	1.158×10^{-4}
0.6×10^{-3}	4.236 ± 0.01	1.176×10^{-2}	1.383×10^{-4}
0.8×10^{-3}	5.87 ± 0.01	1.223×10^{-2}	1.496×10^{-4}
1.0×10^{-3}	7.088 ± 0.02	1.181×10^{-2}	1.395×10^{-4}
1.2×10^{-3}	8.73 ± 0.01	1.212×10^{-2}	1.469×10^{-4}

Table 5c. Diffusion coefficients of Fe(III)-thymoquinone complex at different metal-ligand ratios

L/M Ratio	$I_{pa}\times10^{-5}$ (A)	$D^{1/2}$	D ($cm^2\ s^{-1}$)
1	0.588 ± 0.02	1.96×10^{-3}	3.84×10^{-6}
2	0.919 ± 0.01	3.063×10^{-3}	9.38×10^{-6}
3	1.035 ± 0.01	3.449×10^{-3}	1.19×10^{-5}
4	1.187 ± 0.03	3.956×10^{-3}	1.565×10^{-5}
L/M Ratio	$I_{pc}\times10^{-5}$ (A)	$D^{1/2}$	D ($cm^2\ s^{-1}$)
1	1.149 ± 0.01	3.829×10^{-3}	1.466×10^{-5}
2	2.683 ± 0.02	8.941×10^{-3}	7.995×10^{-5}
3	4.084 ± 0.01	1.36×10^{-2}	1.852×10^{-4}
4	5.002 ± 0.02	1.67×10^{-2}	2.779×10^{-4}

Cyclic voltammetric study of Fe(III)-thymoquinone complex was performed at glassy carbon elelctrode against Standard calomel electrode. Horizontal base line (NaCl) indicates the purity of system. The qualitative and quantitative analyses were performed for this complex. Qualitative analysis clearly showed the formation of complex on mixing of Fe(III) and thymoquinone. Quantitative analyses included determination of E°, D, α and β. Effects on complexation were observed at different parameters. Present research reveals that calibration curve method by cyclic voltammetry can be used for quantification of this complex. Effect of repeated scanning on cyclic voltammograms showed no pre or post peak indicating no adsorption of the complex on electrode surface. E° being a characteristic property is constant for a particular system. In present study, effects of scan rate, concentration and ratio were observed on E° and it was found to be constant in all above mentioned cases. Diffusion coefficient was calculated using Randles- Sevick equation. The values of transfer coefficients, α and β were also determined by varying scan rates and metal ligand ratios.

Table 6. Half wave potential ($E^\circ = E_{1/2}$) for Fe(III)-thymoquinone complex

Scan rates (ν) V/s	$(E^\circ)_a$ (V)	Conc. $\times10^{-3}$ M	$(E^\circ)_a$ (V)	Ratio LM	$(E^\circ)_a$ (V)
0.05	0.274 ± 0.01	0.1	0.195 ± 0.01	1	0.256 ± 0.01
0.10	0.286 ± 0.01	0.2	0.237 ± 0.01	2	0.27 ± 0.01
0.15	0.292 ± 0.01	0.4	0.266 ± 0.01	3	0.285 ± 0.01
0.20	0.297 ± 0.01	0.6	0.295 ± 0.01	4	0.296 ± 0.02

Electrochemical study revealed quasi-reversible behaviour for Fe(III)-thymoquinone complex. It was supported by diagnostic criteria for a quasi-reversible reaction (Table 3).

References

Abdelmeguid, E.N., Fakhoury, R., Kamal, S.M., Al Wafai, R.J. 2010. Effect of *Nigella sativa* and thymoquinone on biochemical and subcellular changes in pancreatic β-cells of streptozotocin induced diabetic rats. *Journal of Diabetes*, **2:** 256-266.

Ali, B.H., Blunden, G. 2003. Pharmacological and toxicological properties of *Nigella sativa*. *Phytotherapy Research*, **17:** 299-305.

Ali, S.A. 1995. Electrochemical Studies of Some Biologically Active Compounds using Graphite Paste Electrode, *Ph.D. Thesis*, pp. 223-240, University of Karachi, Karachi, Pakistan.

Al-Shabanah, O.A., Badary, O.A., Nagi, M.N., Al-Gharably, N.M., Al-Rikabi, A.C., Al-Bekairi, A.M. 1998. Thymoquinone protects against doxorubicin-induced cardio-toxicity without compromising its antitumor activity. *Journal of Experimental Clinical Cancer Research*, **17:** 193-198.

Anwer, H. 2006. Complexation of Vanadyl Compounds with Maltol, *Ph.D. Thesis*, pp. 235-240, University of Karachi, Karachi, Pakistan.

Badary, O.A., Abd-Ellah, M.F., El-Mahdy, M.A., Salama, S.A. Hamada, F.M. 2007. Anticlastogenic activity of thymoquinone against benzo (a) pyrene in mice. *Food and Chemical Toxicology*, **45:** 88-92.

Badary, O.A., Taha, R.A., Gamal el-Din, A.M., Abdel-Wahab, M.H. 2003. Thymoquinone is a potent superoxide anion scavenger. *Drug and Chemical Toxicology*, **26:** 87-98.

Badary, O.A., Al-Shabanah, O.A., Nagi, M.N., Al-Rikabi, A.C. Elmazar, M.M. 1999. Inhibition of benzo (a) pyrene- induced forestomach carcinogenesis in mice by thymoquinone. *European Journal of Cancer Prevention*, **8:** 435-440.

Bard, A.J., Faulkner, L.R. 2001. *Electrochemical Methods: Fundamentals and Applications*, pp. 239-243, 2nd edition, John Wiley and Sons (Asia), Singapore, NY, USA.

Cotton, F.A., Wilkinson, G. 1988. *Advanced Inorganic Chemistry*, pp. 710-713, 5th edition, John Wiley & Sons, New York, USA.

Dockal, E.R., Cass, Q.B., Brocksom, T.J., Brocksom, U., Correa, A.G. 1955. A simple and efficient synthesis of thymoquinone and methyl-p-benzoquinone. *Synthetic Communications*, **15:** 1033-1036.

Eleanor, N.W., Sharon, R.R. 2002. *Understanding Nutrition*, 430 pp., 9th edition, Wadsworth, Belmont, USA.

El-Mahdy, M.A., Zhu, Q., Wang, Q.E., Wani, G., Wani, A.A. 2005. Thymoquinone induces apoptosis through activation of caspase-8 and mitochondrial events in p53-null myeloblastic leukemia HL-60 cells. *International Journal of Cancer*, **117:** 409-417.

Fararh, K.M., Shimizu, Y., Shiina, T., Nikami, H., Ghanem, M.M., Takewaki, T. 2005. Thymoquinone reduces hepatic glucose production in diabetic hamsters. *Research in Vaterinary Science*, **79:** 219-223.

Gali-Muhtasib, H., Ocker, M., Kuester, D., Krueger, S., El-Hajj, Z., Diestel, A., Evert, M., El-Najjar, N., Peter, B., Jurjus, A., Roessner, A., Schneider-Stock, R. 2008. Thymoquinone reduces mouse colon tumor cell invasion and inhibits tumor growth in murine colon cancer models. *Journal of Cellular and Molecular Medicine*, **12:** 330-342.

Gazzar, M.A., El Mezayen, R., Nicolls, M.R., Dreskin, S.C. 2007. Thymoquinone attenuates proinflammatory responses in lipolysaccharide-activated mast cells by modulating NF-kappa B nuclear transactivation. *Biochimica et Biophysica Acta*, **1770:** 556-564.

Greef, R., Peat, R., Peter, L.M., Pletcher, D., Robinson, J. 1985. *Instrumental Methods in Electrochemistry*, pp. 183-188, 1st edition, John Wiley and Sons, New York, USA.

Hosseinzadeh, H., Eskandari, M., Ziaee, T. 2008. Antitussive effect of thymoquinone, a constituent of *Nigella sativa* seeds, in guinea pigs. *Pharmacology online*, **2:** 480-484.

Housecroft, C.E., Sharpe, A.G. 2005. *Inorganic Chemistry*, pp. 590-594, 2nd edition, Longman Singapore Publishers (Pvt) Ltd, Singapore, Pearson Prentice Hall, England, UK.

Mansour, M.A., Nagi, M.N., El-Khatib, A.S., Al-Bekairi, A.M. 2002. Effects of thymoquinones on antioxidant enzyme activities, lipid peroxidation and DT-diaphorase in different tissues of mice: a possible mechanism of action. *Cell Biochemistry and Function*, **20:** 143-151.

Mehta, B.K., Pandit, V., Gupta, M. 2009. New principles from seeds of *Nigella sativa*. *Natural Product Research*, Part A, **23:** 138-148.

Michelitsch, A., Rittmannsberger, A., 2003. A simple differential pulse polarographic method for the determination of thymoquinone in black seed oil. *Phytochemical Analysis*, **14:** 224-227.

Mohamed, A., Shoker, A., Bendjelloul, F., Mare, A., Alzrigh, M., Benghuzzi, H., Desin, T. 2003. Improvement of experimental allergic encephalomyelitis (EAE) by thymoquinone; an oxidative stress inhibitor. *Biomedical Sciences Instrumentation*, **39:** 440-445.

Mouhajir, F., Pedersen, J.A., Rejdali, M., Towers, G.H.N. 1999. Antimicrobial thymohydroquinones of Moroccan *Nigella sativa* seeds detected by electron spin resonance. *Pharmaceutical Biology*, **37:** 391-395.

Nicholson, R.S. 1965. Theory and application of cyclic voltammetry for measurement of electrode reaction kinetics, *Analytical Chemistry*, **37:** 1351-1355.

Padhye, S., Banerjee, S., Ahmed, A., Mohammad, R., Sarkar, F.H. 2008. From here to eternity- the secret of pharaohs: therapeutic potential of black seeds and beyond. *Cancer Therapy*, **6:** 495-510.

Pagola, S., Benavente, A., Raschi, A., Romano, E., Molina, M.A.A., Stephens, P.W. 2004. Crystal structure determination of thymoquinone by high-resolution X-ray powder diffraction. AAPS. *Pharmaceutical Science and Technology*, **5:** 24-31.

Shoieb, A.M., Elgayyar, M., Dudrick, P.S., Bell, J.L., Tithof, P.K. 2003. *In vitro* inhibition of growth and induction of apoptosis in cancer cell lines by thymoquinone. *International Journal of Oncology*, **22:** 107-113.

Syed, A.A. 2008. Thymoquinone protects renal tubular cells against tubular injury. *Cell Biochemistry and Function*, **26:** 374-380.

Xin, X., Xue, H., Ajiaikebaier, A., Wang, H. 2008. Research advances of *Nigella* spp. plants. *Schizhen Guoyi Guoyao*, **19:** 1514-1517.